$T=0$ and $T=1$ states in the odd-odd $N=Z$ nucleus, $^{70}_{35}Br_{35}$

D. G. Jenkins,[1,2,*] N. S. Kelsall,[3] C. J. Lister,[2] D. P. Balamuth,[1] M. P. Carpenter,[2] T. A. Sienko,[2]
S. M. Fischer,[4] R. M. Clark,[5] P. Fallon,[5] A. Görgen,[5] A. O. Macchiavelli,[5] C. E. Svensson,[5] R. Wadsworth,[3]
W. Reviol,[6] D. G. Sarantites,[6] G. C. Ball,[7] J. Rikovska Stone,[8,9] O. Juillet,[10] P. Van Isacker,[10]
A. V. Afanasjev,[2,11,12] and S. Frauendorf[11,13]

[1]*Department of Physics, University of Pennsylvania, Philadelphia, Pennsylvania 19104*
[2]*Physics Division, Argonne National Laboratory, Argonne, Illinois 60439*
[3]*Department of Physics, University of York, Heslington, York YO1 5DD, United Kingdom*
[4]*Department of Physics, DePaul University, Chicago, Illinois 60614*
[5]*Nuclear Science Division, Lawrence Berkeley National Laboratory, Berkeley, California 94720*
[6]*Department of Chemistry, Washington University, St. Louis, Missouri 63130*
[7]*TRIUMF, 4004 Wesbrook Mall, Vancouver, British Columbia, Canada V6T 2A3*
[8]*Clarendon Laboratory, Department of Physics, University of Oxford, Oxford OX1 3PU, United Kingdom*
[9]*Department of Chemistry and Biochemistry, University of Maryland, College Park, Maryland 20742*
[10]*Grand Accélérateur National d'Ions Lourds, Boîte Postale 55027, F-14076 Caen Cedex 5, France*
[11]*Department of Physics, University of Notre Dame, Notre Dame, Indiana 46556*
[12]*Laboratory of Radiation Physics, Institute of Solid State Physics, University of Latvia, LV 2169 Salaspils, Miera str. 31, Latvia*
[13]*IKH, Rossendorf Research Centre, PB 51 01 19, D-01314 Dresden, Germany*

(Received 18 January 2002; published 28 May 2002)

Excited states in ^{70}Br were populated in the ^{40}Ca(^{32}S,pn) reaction at $E_{beam}=80$–100 MeV and the ^{40}Ca(^{36}Ar,αpn) reaction at $E_{beam}=145$ MeV. The resulting gamma decay was detected using the Gammasphere array triggered by a 30-element neutron detector. The cross-bombardment allowed the unambiguous assignment of levels to ^{70}Br, comprising a total of 32 states built both on the $J^{\pi}=0^{+}$ ground state and a previously known $J^{\pi}=9^{+}$ isomer, which is located at an excitation energy of 2293 keV by the observation of linking transitions. The structures are discussed within the context of the two-quasiparticle plus rotor model, the IBM-4 model and the cranked Nilsson-Strutinsky formalism. The nonobservation of a doublet of $J=0$, $T=1$ and $J=1$, $T=0$ states at low excitation in ^{70}Br is indicative that $T=0$ proton-neutron pairing strength is weak in comparison to $T=1$ pairing.

DOI: 10.1103/PhysRevC.65.064307 PACS number(s): 21.10.Hw, 21.10.Re, 23.20.Lv, 27.50.+e

I. INTRODUCTION

Self-conjugate $N=Z$ nuclei are an ideal place to study nuclear wave functions and correlations due to their high degree of symmetry. In particular, in medium-mass odd-odd $N=Z$ nuclei, two symmetries coexist near the ground state, with particles coupled either with space/spin symmetry and isospin antisymmetry ($T=0$ states) or with space or spin antisymmetry and isospin symmetry ($T=1$ states). The relative positions of these sets of states and the location of their spin-dependent multiplets can tell us a great deal about both long- and short-range neutron-proton correlations, and about the shape of the nuclear mean field. However, a rather complete identification of these states, including levels of both low and high spin, and with their inferred isospin, is necessary for a comprehensive analysis that would give a clear-cut picture of shape, symmetries, and residual interactions between valence particles.

In addition to their structural interest, these nuclei lie along the explosive rp-process nucleosynthesis path. The bulk properties of these nuclei such as their masses, half-lives, shapes, and isomers can have a strong influence on modeling the rp-process and identifying its possible nucleosynthesis sites. Finally, the ground-state beta-decays of the odd-odd nuclei are superallowed Fermi transitions which can be used to test the conserved vector current (CVC) hypothesis of β decay and to search for new physics beyond the standard model. However, for such precise investigations, small nuclear structure-dependent corrections are needed. Detailed spectroscopic information can help test the reliability of these corrections.

The structure of odd-odd $N=Z$ nuclei in the fp shell for example, ^{46}V [1,2], ^{50}Mn [3], and ^{54}Co [4], has been studied in some detail. A complete spectroscopic picture of these nuclei is greatly facilitated by the possibility of probing high spin states by heavy-ion fusion evaporation reactions and nonyrast low spin states by $(p,n\gamma)$ reactions. Very strong $\Delta T=1$ $M1$ transitions have been seen with some of the largest $B(M1)$ values known which have been attributed to quasideuteron configurations [1,3,4]. These enhanced $M1$ decays stand in contrast to the inhibited isoscalar $\Delta T=0$ $M1$ transitions in $N=Z$ nuclei [5], and, hence, serve as a useful tool for classifying the relative isospin of states. From a theoretical standpoint, the low-lying structure of these fp-shell nuclei is readily modeled by large-scale shell model calculations.

*Present address: Oliver Lodge Laboratory, University of Liverpool, Liverpool L69 3BX, United Kingdom.

By contrast, the structure of odd-odd $N=Z$ nuclei in the mass 60-90 region is relatively unexplored. Experimentally, the nuclei are far more difficult to study than the fp shell nuclei, since they lie much further away from the line of stability, approaching the proton drip line, and have production cross sections two orders of magnitude lower than in the fp shell. There are no stable targets available for use in $(p,n\gamma)$ studies. Heavy-ion fusion-evaporation reactions (or in some special cases, fragmentation reactions) must be employed, which are not normally well suited for the complete spectroscopy which is needed. The spectroscopy of odd-odd $N=Z$ nuclei above $A=58$ is therefore at the limits of present sensitivity even with the largest arrays of germanium detectors. Theoretically, an interpretation of the structure of these nuclei is hindered by the fact that most of them lie beyond the scope of even the largest basis shell model calculations presently possible, so more approximate approaches must be tried. The heaviest $N=Z$ nucleus for which shell model calculations presently exist is ^{62}Ga [6], although Monte Carlo shell model approaches are being developed to probe the structure of heavier nuclei [7,8]. Study of odd-odd $N=Z$ nuclei in the mass 60-90 region is, accordingly, both an experimental and theoretical challenge at the limit of present techniques.

II. STATE OF KNOWLEDGE OF THE ODD-ODD $N=Z$ NUCLEI BEYOND ^{56}Ni

The opportunity for extending precise tests of CVC theory of superallowed beta decay to $N=Z$ nuclei above $A=60$ is now approaching. Producing a sufficient quantity of these radioactive nuclei, through fusion, spallation, or fragmentation, and rapidly transferring them to ion traps for accurate mass measurements is now feasible, and first results are imminent for ^{74}Rb. Preliminary lifetimes have been measured to $A=96$ [9,10], and a lifetime measurement at the necessary level of precision has now been made for ^{74}Rb [11,12]. High-quality investigations of the fragmentation of the β-decay strength, and a detailed investigation of the low-lying structure of the parent and daughter nuclei, are also needed.

At the onset of this work, no gamma-emitting excited states were known in ^{70}Br. Recently, first results have been published on excited states in ^{58}Cu [13], ^{62}Ga [6], ^{66}As [14,15], ^{74}Rb [16], and ^{78}Y [17]. The present investigation on ^{70}Br completes the cycle of ''identification'' studies of these odd-odd systems. ^{70}Br is known to have a $T=1$, $J^{\pi}=0^{+}$ ground state with a $T_{1/2}=79.1(8)$ ms lifetime [18]. A longer-lived $T_{1/2}=2.2(2)$ s β-decaying isomer has been known for some years [19]. Recently, an analysis of the isomer decay to known states in ^{70}Se allowed the spin and parity to be firmly established as $J^{\pi}=9^{+}$ [20,21]. However, these decay studies did not determine the excitation energy of the isomer in ^{70}Br. Prior to this work, states in ^{70}Br were postulated [22], but later retracted [23]. Thus the present study was aimed at rigorously identifying the structures based on the ground state and the isomer, and at establishing the excitation energy of the isomer above the ground state.

During the final preparation of this paper a more restricted and lower statistics study of ^{70}Br was published by de Angelis *et al.* [24]. The present work is in agreement with their assignment of the strongest transitions in the low-spin portion of our level scheme. However, we find there are discrepancies between the experiments concerning some of the weaker transitions. These transitions are of critical importance to their interpretation of the data. Consequently, we have added a short section to discuss these differences and their consequences.

III. EXPERIMENTAL DETAILS AND DATA REDUCTION

We have identified excited states in ^{70}Br in two separate reactions and using two different identification techniques, both using Gammasphere to maximize the efficiency for detecting gamma rays. The cross-bombardment and variety of experimental methods employed makes the assignment of transitions to the decay of states in ^{70}Br unambiguous. Further, it allows us clearly to differentiate excited states built on the ground state from those built on the high-spin isomer.

For the low-spin investigation the ^{40}Ca(^{32}S,pn)^{70}Br reaction was used at beam energies of 80, 85, 90, and 100 MeV. Most of the data were collected at the 88 Inch Cyclotron at Berkeley, using a backed target consisting of 400 μg/cm^2 of ^{40}Ca with a 120-μg/cm^2 flash of gold on the front and a 15-mg/cm^2 molybdenum backing. The backing was chosen to minimize the yield of X rays in the 20–100-keV region in order to allow a search for low-energy gamma rays in ^{70}Br. The target backing stopped the residual nuclei, allowing a search for additional isomers in the 1–100-ns regime. Gammasphere was operated in its recently implemented ''leading-edge'' timing mode to enhance the triggering efficiency for low-energy gamma rays. In addition, five Gammasphere detector modules were removed from the ring of detectors at 57° and replaced with large area low-energy photon spectrometer (LEPS) planar detectors, located 15 cm from the target, to enhance timing and energy resolution for low-energy radiation. The LEPS array had an efficiency of $\sim$2% at 122 keV. A small, thin-walled chamber was used, again to improve sensitivity to low-energy radiation. Thirty downstream Gammasphere detector modules were removed and replaced with BC501 liquid scintillator neutron detectors, to provide a 25% efficient 'neutron' fast trigger which suppressed the very intense charged-particle reaction channels. The remaining 69 Compton suppressed modules were measured to have 6% photopeak efficiency at 1.33 MeV. The neutron signal, in coincidence with any one of the remaining 69 Compton-suppressed Gammasphere detectors, or a LEPS detector, initiated an event readout.

The excitation function provided very useful information. At the lowest beam energy (80 MeV), which was below the classical Coulomb barrier for ^{32}S+^{40}Ca, gamma rays associated with reaction products from the ^{72}Kr compound nucleus were all very low in intensity. In contrast, a considerable flux of gamma rays was observed from reactions on contaminant materials, particularly from ^{32}S+^{16}O from oxidation of the target and ^{32}S+^{12}C from cracking hydrocarbons onto the target. The yield of the gamma rays associated with contaminants increased monotonically and slowly with

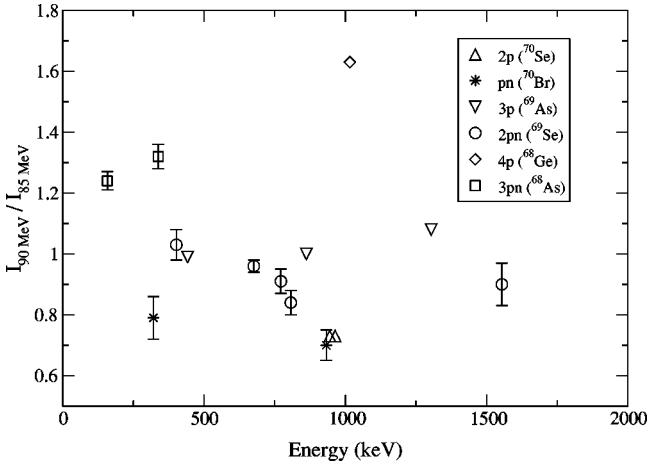

FIG. 1. Plot of the ratio of the intensity of gamma rays associated with different exit channels in the $^{32}S+^{40}Ca$ reaction at beam energies of 90 and 85 MeV. Candidate transitions for ^{70}Br as well as representative transitions associated with other exit channels are shown. The ratio has been normalized with respect to the 862-keV gamma ray in ^{69}As produced via the three-proton evaporation channel.

beam energy, whereas the gamma rays from reaction products associated with the $^{32}S+^{40}Ca$ reaction changed rapidly, especially near the Coulomb barrier. The two-particle evaporation channels $2p$, pn, and $2n$ had a unique excitation function: they peaked near 85 MeV, and fell at higher energies as multiparticle evaporation became favorable. The $2p$ channel led to well-known ^{70}Se. The suppression of ^{70}Se transitions in software-gated ''neutron'' spectra was used to evaluate the quality of neutron discrimination. The suppression of non-neutron-emitting channels was found to be $>5\times10^3$. Transitions in ^{70}Br had the same excitation function as ^{70}Se lines, but were not suppressed in ''neutron-gated'' spectra. In this manner, candidate gamma rays were identified (see Fig. 1). In principle, ^{70}Kr transitions should be enhanced in neutron-gated data, and be unique in double-neutron gated spectra. However, despite a careful search no unambiguous candidates were found, probably implying a production cross section of less than 1 microbarn. The population of states in ^{70}Se was used as a monitor to evaluate the two-nucleon evaporation residue entry spin distribution directly. At 85 MeV the mean angular momentum in ^{70}Se was measured to be $\langle J\rangle \sim 6\hbar$, and the highest observed state had $J=10\hbar$. Most of the data were collected at this energy. A similar spin distribution was expected for ^{70}Br, so the conditions were ideal for populating low-spin states based on the ground state, and avoiding the population of states based on the 9^+ isomer. In practice, despite a careful optimization of experimental conditions, no low-energy transitions below 300 keV were observed in ^{70}Br, nor states with intermediate isomeric lifetimes on the 1–100 ns scale.

A second study, examining the $^{40}Ca(^{36}Ar,\alpha pn)^{70}Br$ reaction at 145 MeV, using beams from the Argonne ATLAS accelerator, was more conventional and focused on higher angular momentum states, based both on the ground state and isomer. A mean residue angular momentum of $\langle J\rangle \sim 20\hbar$ was predicted. In this experiment the target was again 400 μg/cm^2 ^{40}Ca, but with 100 μg/cm^2 of gold on the front and back. The ''Microball'' detector, consisting of 95 CsI detectors, was used to detect light charged particles [25], and the 30 detector neutron shell was once more used, leaving 73 Gammasphere detector modules. The trigger condition was one scintillator and at least two Compton-suppressed germanium detectors, or more than four Compton-suppressed germanium detectors.

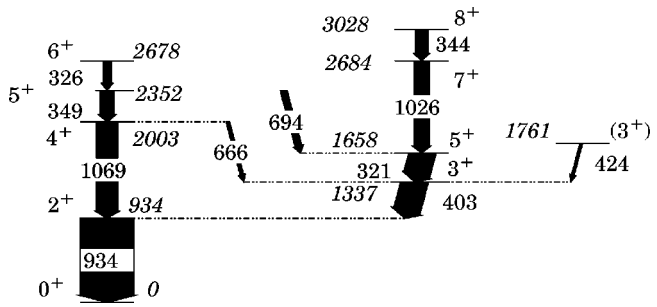

FIG. 2. Low-spin level scheme for ^{70}Br with information derived solely from the ^{32}S study. The width of the arrows corresponds to the intensity of the transition.

In the latter study, ^{70}Br was identified by detecting all the evaporated particles, that is, exactly one alpha particle, one proton, and one neutron. Gamma-gamma coincidence matrices in good time coincidence with this combination of particles were created. This selection also admitted higher particle multiplicity reactions, like $^{40}Ca(^{36}Ar,2\alpha pn)^{66}As$, $^{40}Ca(^{36}Ar,\alpha 3pn)^{68}As$, and $^{40}Ca(^{36}Ar,\alpha 2pn)^{69}Se$. However, these reactions could be individually selected by suitable particle gating then carefully subtracted from the matrix generated with only the single alpha particle, proton, and neutron gating conditions. Fortunately, the residues from higher fold particle channels were recently studied [26,27], so the removal of gamma rays associated with such breakthrough channels could be effectively monitored. Once candidate transitions were identified, the channel selection was enhanced by determining the optimal region in the total-energy plane (TEP) associated with ^{70}Br by setting gates on pairs of the candidate transitions [28]. This technique relies on the total charged particle energy detected being larger for true αpn events compared to those from higher fold channels, where one or more of the emitted charged particles evaded detection. The various ^{70}Br candidate gamma-ray cascades were all found to be associated with a near-identical region in the total-energy plane, further supporting the hypothesis that they all originated from the same reaction channel.

Following the identification of gamma ray transitions in ^{70}Br, level schemes for states built on the $J^\pi=0^+$ ground state as well as the 9^+ isomer were produced from an analysis of double and triple coincidences with these candidate transitions in both data sets. The level scheme derived from the ^{32}S reaction is presented in Fig. 2 and a composite of the information obtained from both reactions is presented in Fig. 3. In order to determine multipolarities for the observed gamma rays, an angular correlation analysis was performed. For each data set, matrices were sorted of all detectors

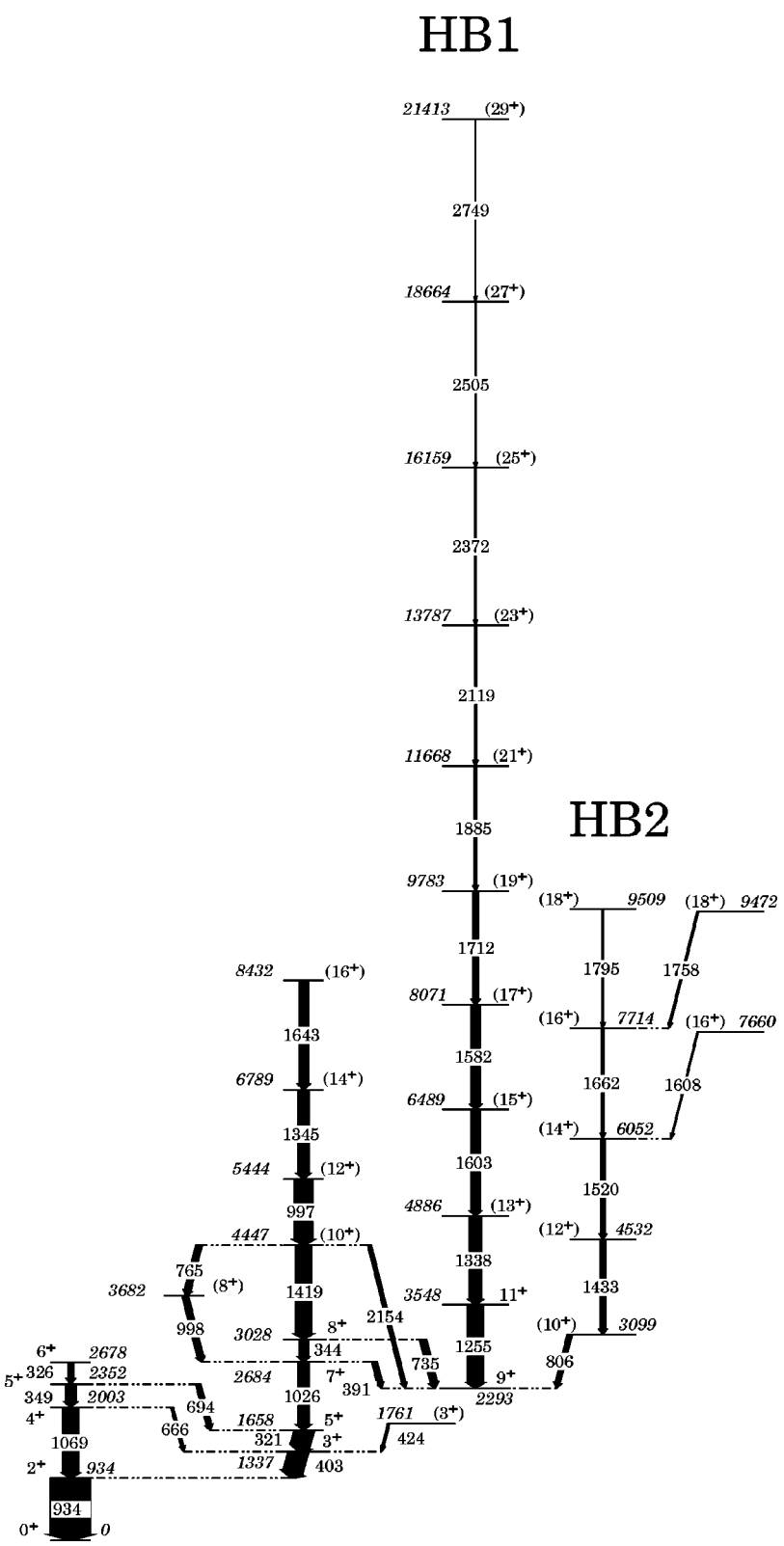

FIG. 3. Composite level scheme for ^{70}Br. The width of the arrows corresponds to the intensity of the transition. The intensities are a composite of the intensities from the two studies related to each other by the intensity of the 403-keV transition (see the text).

against those at backward angles greater than 120°, and of all detectors against those at angles between 79° and 101°. Gating on the all detector axis in each case, the ratio of the intensity of transitions in the two matrices was obtained. By studying transitions of well-established multipolarity in strongly populated channels by this method, it was deduced that a ratio of approximately 0.5 corresponded to a pure dipole transition, while a ratio of 0.9 corresponded to a stretched quadrupole transition. The results of this angular correlation analysis as well as the energies and intensities of ^{70}Br gamma rays from both data sets are presented in Table I.

TABLE I. Energies, intensities, and angular correlation ratios from both data sets. The intensities from the two data sets have been normalized such that the 403 keV has 100%. The energies marked with † are an average of the measured energies from the two data sets. These were consistent within experimental errors. Doublets are marked with ‡. The quoted intensity is for the doublet. ◇ A search was made for the 391-keV transition in the ^{32}S data set, where it would be expected to be in coincidence with the 344-keV line. Unfortunately, the presence of a very strong 344–391-keV coincidence in a contaminant (^{68}As) precluded its confirmation.

Energy (keV)	I_γ ^{40}Ca(^{36}Ar, αpn)	I_γ ^{40}Ca(^{32}S, pn)	R_{corr} ^{40}Ca(^{36}Ar, αpn)	R_{corr} ^{40}Ca(^{32}S, pn)	Assignment
320.7(3)†	97(12)	52(6)	0.93(15)	0.90(12)	$5^+ \rightarrow 3^+$
326.1(3)	-	30(6)		0.31(9)	$6^+ \rightarrow 5^+$
344.4(5)	46(5)	9(3)	0.52(14)		$8^+ \rightarrow 7^+$
348.6(4)	-	51(6)		0.47(16)	$5^+ \rightarrow 4^+$
390.7(4)	27(4)	◇			$7^+ \rightarrow 9^+$
402.6(3)†	≡100	≡100	0.76(9)	0.52(14)	$3^+ \rightarrow 2^+$
424.0(5)	-	10(3)			$(3^+) \rightarrow 3^+$
665.7(3)	-	13(3)			$4^+ \rightarrow 3^+$
694.0(4)	-	25(4)			$5^+ \rightarrow 5^+$
734.8(4)	35(6)	-			$8^+ \rightarrow 9^+$
765.0(4)	31(5)	-	1.00(22)		$(10^+) \rightarrow (8^+)$
806.2(4)	24(3)	-	0.76(8)		$(10^+) \rightarrow 9^+$
933.6(3)†	-	-	0.87(13)		$2^+ \rightarrow 0^+$
997.1(5)	123(9)‡	-	1.18(15)		$(12^+) \rightarrow (10^+)$
998.0(5)	123(9)‡	-	1.18(15)		$(8^+) \rightarrow 7^+$
1026.0(5)†	57(7)	34(6)	-	1.09(25)	$7^+ \rightarrow 5^+$
1068.8(3)	-	78(9)		0.85(10)	$4^+ \rightarrow 2^+$
1254.8(3)	77(4)	-	0.99(15)		$11^+ \rightarrow 9^+$
1337.6(3)	61(4)	-			$(13^+) \rightarrow 11^+$
1344.6(5)	55(6)	-			$(14^+) \rightarrow (12^+)$
1418.6(7)	80(7)	-	0.92(15)		$(10^+) \rightarrow 8^+$
1432.6(5)	27(4)	-			$(12^+) \rightarrow (10^+)$
1519.7(4)	22(3)	-			$(14^+) \rightarrow (12^+)$
1582.4(4)	44(6)	-			$(17^+) \rightarrow (15^+)$
1602.6(4)	47(6)	-			$(15^+) \rightarrow (13^+)$
1608.2(6)	5(1)	-			$(16^+) \rightarrow (14^+)$
1642.8(6)	46(4)	-			$(16^+) \rightarrow (14^+)$
1661.5(5)	12(3)	-			$(16^+) \rightarrow (14^+)$
1712.2(6)	30(5)	-			$(19^+) \rightarrow (17^+)$
1758.0(5)	8(2)	-			$(18^+) \rightarrow (16^+)$
1795.0(6)	7(2)	-			$(18^+) \rightarrow (16^+)$
1885.0(6)	12(3)	-			$(21^+) \rightarrow (19^+)$
2118.9(7)	9(2)	-			$(23^+) \rightarrow (21^+)$
2155.0(12)	18(3)	-			$(10^+) \rightarrow 9^+$
2371.7(11)	5(2)	-			$(25^+) \rightarrow (23^+)$
2505.0(13)	3(1)	-			$(27^+) \rightarrow (25^+)$

IV. ANALYSIS

The development of decay schemes of odd-odd nuclei is never easy, as the two unpaired particles at the Fermi surface can lead to a large number of states at a relatively low energy. In the vicinity of ^{70}Br this situation is expected to be further complicated by shape coexistence, which leads to the possibility of an even greater variety of states, and to the presence of fp- and g-shell model orbits which can give rise to both positive and negative parity structures. Thus considerable caution is needed when making assignments. Only isobaric analog symmetry, which demands a manifold of $T=1$ states in ^{70}Br to match levels in ^{70}Se, can help with the daunting task.

A cascade of five transitions of 321-344-403-934-1026 keV was found in both data sets—Fig. 4 (top) shows this cascade clearly. As the cascade was populated in the experiment using the ^{32}S beam where the input angular momentum was empirically determined to be low, the sequence must be

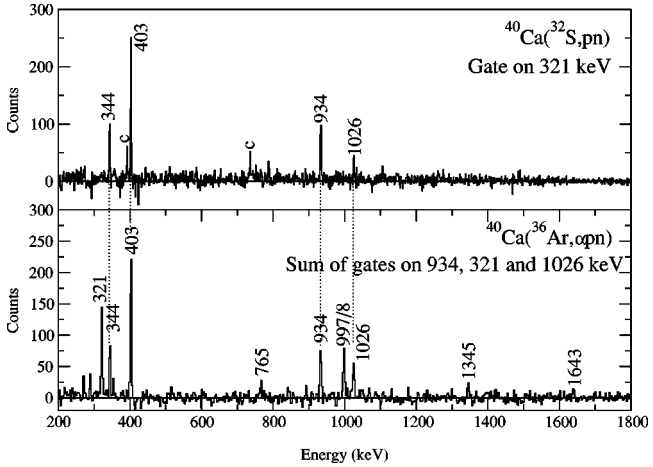

FIG. 4. (Top) Gamma ray spectrum of transitions decaying to the 0^+ ground state from a gate on the 321-keV transition with a condition that one neutron was detected, from the data obtained from the ^{40}Ca(^{32}S,pn) reaction at 90 MeV. Contaminant gamma rays in ^{68}As introduced by the presence of a low-lying 321 keV in the ^{68}As decay scheme [27] are marked with a *c*. (Bottom) A sum of gates on the 934-, 321-, and 1026-keV transitions taken from the ^{40}Ca(^{36}Ar,αpn) data. A particle condition of one proton, one alpha, and one neutron was employed as well as a two-dimensional window in the total-energy plane (see the text). Transitions observed in both data sets are shown with a dotted line joining the two spectra.

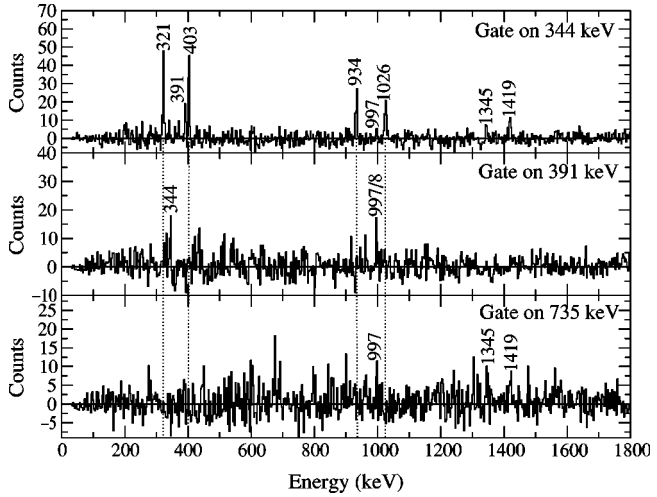

FIG. 5. (Top) Gamma ray spectrum gated on the 344-keV transition. (Middle) Gamma ray spectrum gated on the 391-keV transition. (Bottom) Gamma ray spectrum gated on the 735-keV gamma ray. All the spectra are derived from the ^{40}Ca(^{36}Ar,αpn) data set. In each case a particle gating condition of one alpha, one proton, and one neutron was set, in addition to a two-dimensional gate in the total-energy plane.

associated with the ground state and not the high spin isomer known from beta decay. The most intense of these transitions is a 934-keV gamma ray which we associate with the decay of the analog of the first excited state in ^{70}Se which lies at 945 keV. Gating on this transition reveals the main cascade, and a separate cascade of 326-349-1069 keV γ rays. The strongest transition is of 1069 keV, again a close analog to the ^{70}Se $4^+ \rightarrow 2^+$ transition of 1093 keV. Cross-linking decays of 666 and 694 keV fix the order of the two cascades, an arrangement which is confirmed by intensity balances, and is shown in Fig. 2. Assuming the analog assignments have been made correctly, and with the present angular correlation measurements, a plausible set of spin and parity assignments can be made, which are consistent with most conventional criteria. For example, the nonobservation of a decay from the suggested $J^\pi = 7^+$ state at 2684 keV to the second $J^\pi = 5^+$ state at 2352 keV can be explained by the phase space arising from competition between 332- and 1026-keV $E2$ transitions, which should have the lower-energy transition disfavored by a factor 281. Some puzzles remain which can guide in interpretation. For example the $J^\pi = 7^+$ state has two $E2$ decays; the 1026-keV transition should dominate the 391 keV decay by a factor of 75 if the matrix elements were equal and the transition rates governed solely by phase space and spin factors. In fact they differ only by a factor of 2, indicating that these matrix elements actually differ by a factor of 30. While nothing in the present data rigorously excludes the assignment of negative parity to some of these states, it is tempting to associate them with the expected even-spin, even-parity $T=1$ sequence, and its opposite symmetry partners with odd spin, even parity, and $T=0$.

In the future, one of the best ways to test this hypothesis is to measure the lifetimes of some of these states and extract the interband $M1$ matrix elements. As pointed out by Lisetskiy *et al.* [29], these matrix elements are very sensitive to the symmetry of the wave functions and to deformation, and so can be a most revealing probe, as the matrix elements can span a wide range from $\sim 10^{-3}\mu_N$ to $\sim 10\mu_N$. At present, only one rather indirect test of $M1$ strength can be made. Lifetime measurements have been made for the ^{70}Se analog states [30], so assuming that the $E2$ matrix elements are approximately isospin independent, the branching ratio of the 2003-keV state can be used to extract an upper limit for the $\Delta J = 1$, $4^+ \rightarrow 3^+$, $M1$ decay. A value of < 0.002 W.u. is obtained—a rather small matrix element indicating considerable inhibition, and certainly inconsistent with large $g_{9/2}$ amplitudes in the wave functions of these low-lying states.

The ^{36}Ar-induced experiment allowed the extension of the ground state sequence to higher spin. A further cascade of five gamma rays was observed, in coincidence with the ground-state cascade, as can be seen in Fig. 4 (bottom). The lower members of this cascade were consistent with a dipole and quadrupole transition, which would suggest a spin $J = 10$ state at 4447 keV if the sequence corresponds to a normal ''stretched'' cascade following high-spin heavy-ion reactions. Gating on the highest members of the sequence is very revealing: a bypass path is found which helps to determine the ordering of the lower transitions, but more importantly there are three new transitions seen at 391, 735, and 2154 keV (see Fig. 5). Examination of individual coincidence gates allows these new transitions to be placed. They all appear to terminate on the same state at 2293 keV. Although more than half of the flux coming from high spin feeds this state, no evidence of gamma rays de-exciting the state could be seen. Thus it is highly likely that the state is isomeric, with a lifetime which is greater than 30 ns—the time for ions to fly away from the target position in the

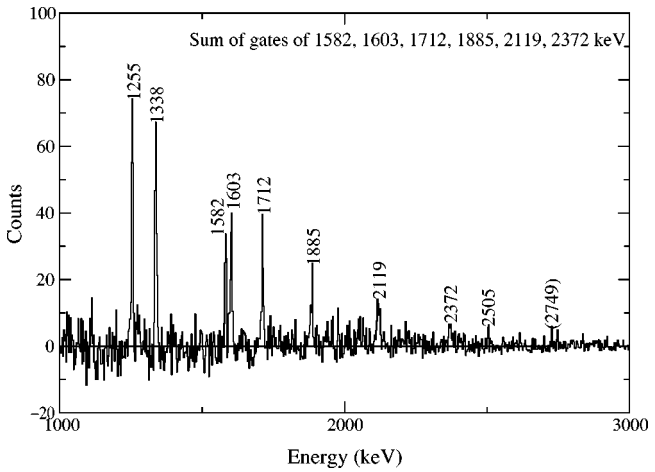

FIG. 6. Gamma ray spectrum for band HB1 constructed from a sum of gates on the 1582-, 1603-, 1712-, 1885-, 2119-, and 2372-keV transitions. The spectrum was taken from the ^{40}Ca(^{36}Ar,αpn) data set with a particle gating condition of one alpha, one proton, and one neutron, and a two-dimensional gate in the total-energy plane.

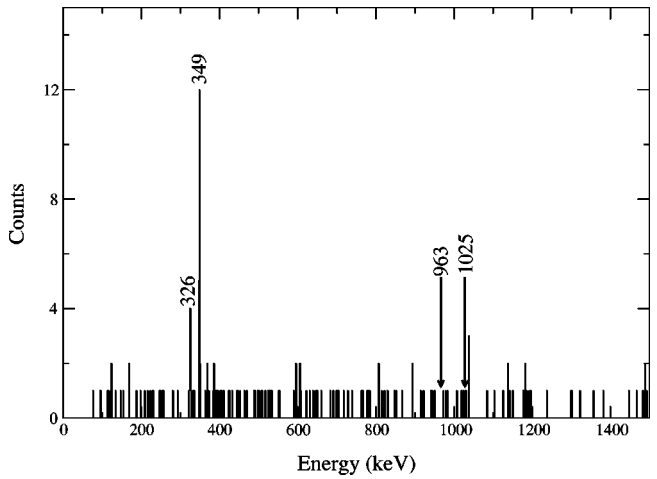

FIG. 7. Gamma ray spectrum double gated on the 933- and 1068-keV transitions. The data are derived from the ^{40}Ca(^{32}S,pn) reaction at 90 MeV. The arrows represent the position of transitions suggested by de Angelis [24].

high-spin study. Considering that states decaying to this 2293-keV level have suggested spins of $J=7$, 8, and 10, it is reasonable to propose that the isomeric state at 2293 keV is the known $J^{\pi}=9^{+}$ $T=2.2$ s β-decaying isomer. The fastest electromagnetic decay from the isomer would be an $E4$ transition to the $J=5$ state at 1658 keV. The Weiskopf single-particle estimate for such a decay has a meanlife of 67 s, which would correspond to a 3% gamma branch near the limit of our sensitivity. However, parent and daughter states may have quite different structures, so the gamma decay is probably considerably suppressed relative to the single-particle estimate. We have searched for any evidence of gamma decays from the isomer, and could find none.

The high-spin experiment also revealed further cascades of transitions that were not populated in the low-spin study—the strongest of which is shown in Fig. 6. They closely follow the identification characteristics of the gamma rays associated with the ground-state excitation, both in their relative enhancement under various particle gating, and in their location in the TEP. These cascades are shown in Fig. 3. A careful search was made for possible linking transitions between the two structures at high spin, as this would remove all uncertainty from the scheme and strongly constrain the spin sequence. No candidates were found except for the three transitions that feed the 9^{+} isomer directly. However, the large spin difference of $9\hbar$ between the ground state and the isomer, and the fact that they most probably have markedly different structures, makes it unclear how strong such linking transitions ought to be.

The decay scheme (see Fig. 3) raises two issues of population following heavy-ion reactions. In the low-spin regime, the analogs of the ^{70}Se ground state band are only yrast to spin $J=4\hbar$. Beyond that, other configurations with $g_{9/2}$ components in their wave functions dominate the yrastline. Population of non-yrast states in heavy-ion reactions is extremely difficult, and can only be achieved in special cases at low spin. Increasing the input angular momentum actually decreases the flux passing through the non-yrast configurations, as population of yrast states dominates. Thus, in our high-spin study, only the yrast states in Fig. 3 were observed, and there was no evidence of any population of ^{70}Se analogs above $J=2\hbar$. In the high angular momentum experiment, several cascades were extended to high spin. The sequence based on the isomer always remained yrast, by more than 1 MeV, as the high-spin bands all have similar moments of inertia. However, it is clear that a wide range of structures are populated and that the non-yrast flux bypasses the isomer and proceeds toward the ground state.

V. COMPARISON WITH DE ANGELIS *et al.*

The low-spin experiment reported here is very similar to that of de Angelis *et al.* [24], both in the fact that the same reaction was used and that the beam energy was very similar. The differences in target thickness make the correspondence even closer. Not surprisingly then, the intensities and DCO ratios we both measure (Table I of both this work and of Ref. [24]) correspond rather well for the strongest transitions with intensity $>10\%$ of the 933-keV gamma ray. These observations indicate a very similar entry spin distribution. However, despite the similarities between experiments, we cannot confirm any of the weaker transitions they reported at intensities below 10%. This is difficult to understand, as our data set appears to have an order of magnitude higher statistics, as is apparent from a comparison of our Fig. 4 (top) with Figs. 1a and 1b of Ref. [24].

de Angelis *et al.* report two gamma rays which extend the ground-state sequence—a 963-keV transition and a very weak 1025-keV transition that they were not able to definitively assign [24]. These are interpreted as gamma rays de-exciting 6^{+} and 8^{+} states, respectively, that form analogs of the ^{70}Se ground-state band. We searched in our data for candidate analogs to the ^{70}Se ground-state band with $J>4\hbar$ and found none, presumably as they are so far removed from the

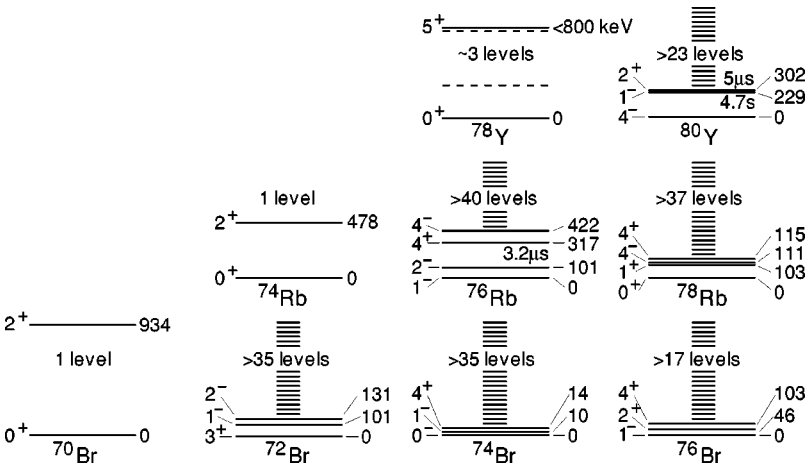

FIG. 8. A comparison of the known levels in the first MeV of excitation energy in neutron deficient odd-odd nuclei in bromine, rubidium, and yttrium isotopes. For the $N=Z$ cases, the level density appears to be unusually low; an effect which does not appear to arise from the lack of experimental sensitivity.

yrast line. Figure 7 shows a spectrum double gated on the 934 ($2^+ \rightarrow 0^+$) and 1069 keV ($4^+ \rightarrow 2^+$) gamma rays in which extensions of the ground-state sequence should be observed. Although the statistics are low, the double-gating procedure is extremely clean. Only two gamma rays with energies of 326 and 349 keV are observed, as expected from our analysis. Scaling from the intensity of these peaks and using the quoted intensities from Table 1 of Ref. [24], we would certainly expect a statistically significant peak at 963 keV and possibly one at 1025 keV to appear in this double-gated spectrum if the analysis suggested by de Angelis *et al.* were correct [24]. In fact the region of interest has an average intensity of 0.1 counts/channel with identically zero counts at the suggested peak position for the $6^+ \rightarrow 4^+$ transition. The gamma-gamma coincidence data afford a similar result, although the Compton backgrounds are higher; where peaks with 30 counts would be expected, no peaks are evident with a statistical limit of <10 counts. In addition to their absence from coincidence spectra, nuclear structure considerations lead us to expect that such ''in-band'' $E2$ decays will not be the dominant decay mode of these $T=1$ states. Indeed, the analog $J=6^+ \rightarrow 4^+$ transition in ^{70}Se has a noncollective $E2$ decay with a $B(E2)$ value of $250e^2\,\mathrm{fm}^4$, due to a shape change from oblate to prolate in the relevant spin region. Therefore, in ^{70}Br, one might expect a dipole decay from the analog 6^+ state to the established $J^\pi=5^+$ state at 1658 keV to be the dominant decay branch as it is strongly favored by phase space. Even a very inhibited $M1$ decay, like the 0.002-W.u. $4^+ \rightarrow 3^+$ decay inferred in the present study, would result in a $>75\%$ decay branch. Such ''dipole dominance'' is well known in odd-odd $N=Z$ fp-shell nuclei where the analog sequences often show no measurable ''in-band'' $E2$ decays [31]. However, an in-band decay is suggested by de Angelis *et al.*, with no mention of evidence for a dipole branch.

de Angelis *et al.* also reported a candidate transition to an isomer with an energy of 1468 keV [24]. Despite the superior statistics in the present work and the fact that high-spin states were favorably populated in the ^{36}Ar-induced study, we find no evidence of such a transition in either data set. It is interesting that we do, however, observe a gamma ray with an identical energy which is a very strong transition in ^{45}Ti produced via the $2pn$ evaporation channel from a reaction with oxygen contamination in the target. Since de Angelis *et al.* marked contaminants from ^{45}Ti on their published spectrum [24], it is clear that this contaminant was strongly populated in their study. This might possibly account for the misassignment of this γ ray. As discussed above, we have a clear candidate in the present work for a $J=9$ isomer which is clearly fed by three gamma rays and whose assignment is entirely consistent with the spins of states which feed it as established from DCO measurements.

In summary, we find no evidence of the $J^\pi=6^+$ and 8^+ states reported by de Angelis *et al.* [24], nor evidence of an isomer fed by a 1468-keV γ ray. Consequently, their discussion concerning Coulomb shifts should be treated with great caution until these states are more rigorously located. This will be experimentally challenging; we could find no candidates for the transitions and believe a much larger data set will be required to locate them as they are very non-yrast and will never be well populated in conventional heavy-ion fusion reactions at any beam energy.

VI. DISCUSSION

A. Empirical observations

Despite a careful search for low-energy gamma rays and isomers, only one level has been identified in ^{70}Br below 1 MeV. This low level density is difficult to attribute to a shortcoming of the heavy-ion reactions used, or lack of experimental sensitivity, as low spin non-yrast bands should have received some population especially in the low-spin study, and the Gammasphere-LEPS combination had sufficient efficiency to reveal transitions with energies more than 20 keV if their intensity was $>10\%$ of the observed 934-keV gamma ray. The lack of low-lying levels stands in sharp contrast to what is known about neighboring odd-odd $N>Z$ nuclei in the region, most of which were investigated by very similar reactions and detectors. On average, the neighbors have more than 30 levels in the first 1 MeV of excitation energy, arranged into more than five rotational-like bands. However, the other odd-odd $N=Z$ nuclei, ^{62}Ga, ^{66}As, ^{70}Br, ^{74}Rb, and possibly ^{78}Y, all seem to have rather few low-lying states, despite having been studied by a variety of techniques [6,14,16,17]. This difference is illustrated in Fig. 8.

While it is true that the $N=Z$ nuclei all have low production cross sections (hundreds of μb), and so it is experimentally difficult to observe poorly populated structures, studies of $N>Z$ odd-odd nuclei revealed quite democratic distributions of population among their bands. Thus it seems that the observed paucity of low-lying states in the odd-odd $N=Z$ nuclei should be taken as a serious indication of special symmetries or interactions involved and not an experimental shortcoming. In our two-quasiparticle plus rotor calculations, discussed in Sec. VI B, we have investigated this issue quantitatively.

One qualitative issue is worthy of mention. In schematic models, for example the recent calculation of Chasman [32], an assumption of equal $T=0$ and 1 pairing strength, leads directly to degenerate $J^{\pi}=0^{+}$, $T=1$ and $J^{\pi}=1^{+}$, $T=0$ low-lying states, in analogy with the parity doublets which arise when mirror symmetry is broken. We have no experimental evidence of a low-lying $J=1^{+}$ state, although we would be quite sensitive to such a level, as there should be strong decays from the 2^{+} and 3^{+} states we have identified. If our present assignments are correct, the first 1^{+} level must lie quite high, above 800 keV, in order to suppress these decay branches to a level below our experimental sensitivity. Thus, taken at face value, this suggests that the $T=0$ pairing strength is substantially weaker than the $T=1$ mode.

Shape coexistence is well documented in the even-even neighbors of ^{70}Br. One manifestation is the observation of bands with very different moments of inertia, the collective oblate shapes have relatively small moments of inertia, and the prolate shapes relatively larger amounts [33]. It is therefore interesting to compare the states we have found with the yrast lines of the even-even neighbors ^{68,70}Se and ^{72}Kr. This comparison is made in Fig. 9. Both ^{68,70}Se are thought to be oblate at low spin. The lowest levels in ^{70}Br also appear to follow this trend. However, above 2 MeV the ^{70}Br states seem to change character and closely follow the ^{72}Kr yrast line, which is thought to be prolate except very near the ground state. Thus, empirically, there seems to be clear evidence of shape coexistence in the structure built on the ground state in ^{70}Br with characteristics similar to its neighbors: oblate at low spin and prolate at higher spins.

The change in moment of inertia at around $J=7$ and $E\sim 2.5$ MeV in the ^{70}Br yrast line suggests a shape change from oblate to prolate (see Fig. 9). Systematic trends in the region suggest that this is the region where $g_{9/2}$ nucleon pairs are expected to break, which may be responsible for driving the shape change. It was noted in Sec. III that in this shape-changing region, the $J=7$ state at 2684 keV exhibits an unusual branching ratio. As will emerge from the following discussion, both decay branches from this state to $J=5$ and 9 states correspond to shape changes, so both decays will probably be inhibited, and with a ratio which is difficult to predict. The fact that the 7^{+} and 9^{+} states probably both have considerable $g_{9/2}$ amplitudes would be consistent with the decay branch connecting these states being the stronger, as observed.

With these data on ^{70}Br, it is possible to examine the systematic trends for all the odd-odd nuclei in the fpg shell

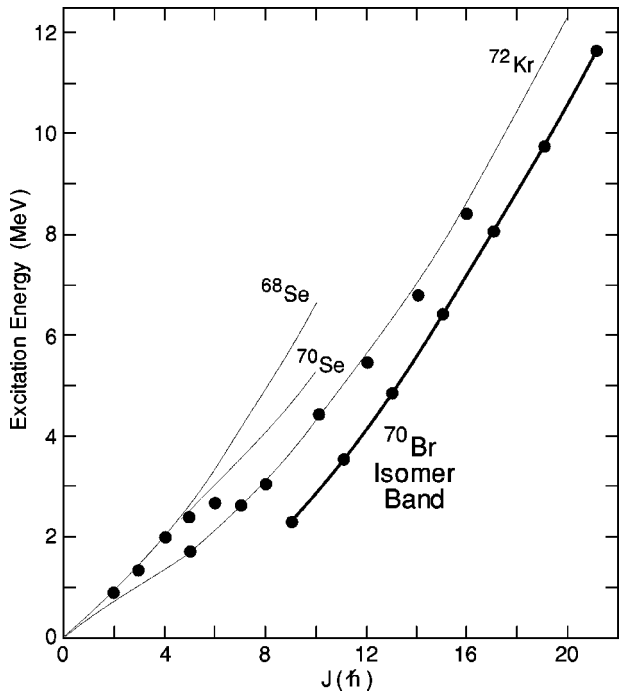

FIG. 9. The location of states in ^{70}Br (dots) in excitation energy and spin, compared to the yrast lines of neighboring even-even nuclei ^{68,70}Se and ^{72}Kr.

from ^{58}Cu to ^{78}Y (see Fig. 10). Despite the wide variety of experimental techniques employed in studying these nuclei, including isomer decay following production in fragmentation reactions, and prompt and delayed spectroscopy following heavy-ion fusion-evaporation reactions, the low-lying states known to date appear remarkably similar. The location and decay of the $J^{\pi}=9^{+}$ state is noteworthy as the shell fills. In ^{62}Ga it is high in excitation (there is a candidate 9^{+} state at 4792 keV) as the $g_{9/2}$ state lies far above the Fermi surface and the 9^{+} state can easily decay to a lower $J=7$ level at 2435 keV. In ^{66}As the $J=9$ state lies at 3024 keV and is isomeric with $T_{1/2}=8.2(5)\mu$s, as the only state to which it can decay is a $J=7$ state only 115 keV below. In ^{70}Br the trend continues, the $J=9$ state falls to 2293 keV which is below the $J=7$ states so it has a long half-life, $T_{1/2}=2.2$ s, and beta decay constitutes its main decay path. The beta decay proceeds entirely to nonyrast states in ^{70}Se [34] despite phase-space considerations which would favor decay to the known prolate yrast $J=8$, and 10 members of the ground-state band. Beyond ^{70}Br, in ^{74}Rb the nuclei have large deformation ($\beta_2=0.4$) prolate ground states, with a low-lying collective rotational band, so the $(g_{9/2})^2$ configuration can once more decay through low multipolarity electromagnetic decays. However, in ^{78}Y, a very low-lying β-decaying isomer with $J^{\pi}=5^{+}$ occurs, based on the $([412]_{5/2})^2$ Nilsson configuration.

Finally, we observe that the sequence of states built on the $J=9$ isomer have, on average, a similar moment of inertia as ^{72}Kr, which can only be associated with a near-prolate shape, as we find in our cranked Nilsson-Strutinsky calculation. The strong cascade of γ rays built on the isomer are initially irregularly spaced, reflecting a change in structure at

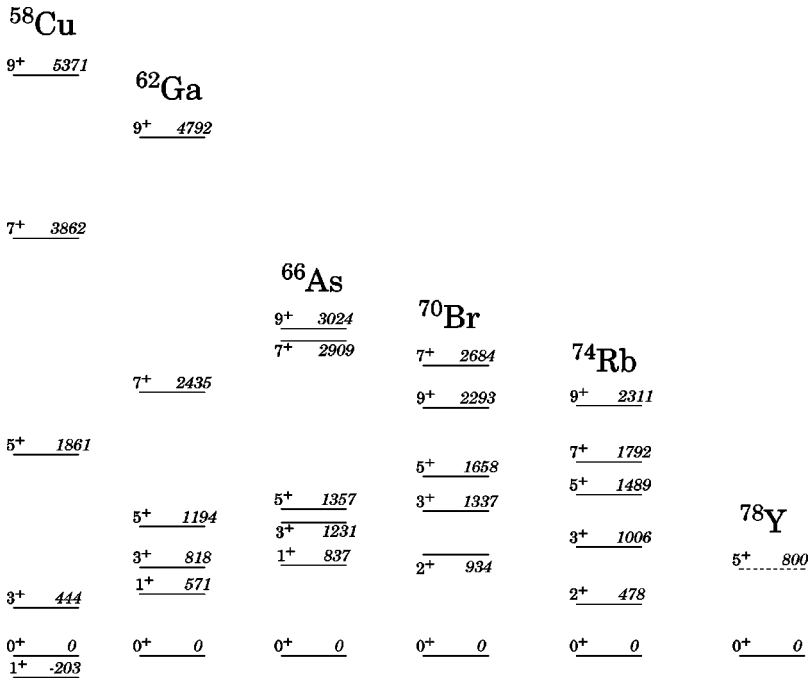

FIG. 10. Comparison of low-lying levels in the odd-odd $N=Z$ nuclei from ^{58}Cu to ^{78}Y. Data are taken from the present work and Refs. [6,13,14,16,17]. In the case of ^{78}Y, the excitation energy of 800 keV for the 5^+ state is an upper limit. In ^{58}Cu the $J=1$ state lies lowest in excitation energy—the spectrum has accordingly been shifted so that the $J=0$ state is aligned with those in the other $N=Z$ nuclei.

relatively close to the band head. Our calculations, presented below, indicate this is a change from oblate to prolate shapes. The isomer-based states are always yrast, by ~ 1 MeV, by virtue of the large band head spin. It must be inferred that the lack of crossing transitions between the high spin structures based on the ground state and the isomer indicates their structures are quite different.

B. Two-particle plus rotor model (TQRM)

Given that ^{70}Br is an odd-odd nucleus, it is highly appropriate to investigate its structure within the two-quasiparticle-rotor model (TQRM) [35,36] where the two quasiparticles are treated explicitly in addition to the collective even-even core. The phenomenological residual interaction between the last unpaired proton and neutron (not to be confused with the much discussed proton-neutron pairing, not present in the TQRM) can be modeled as a zero range delta-force (DF) or finite range central force with a Gaussian radial dependence (CG) [37]. The matrix elements of these interactions are usually fitted to experimental data on excited nuclear levels and are state dependent. No information on matrix elements of the more complicated CG interaction exists in the $A=70$ region, so the simple DF residual interaction in the form [36]

$$V_{pn}=15.75b^3(u_0+u_1\vec{\sigma}_p\cdot\vec{\sigma}_n)\,\delta(\vec{r}_p-\vec{r}_n) \qquad (1)$$

has been adopted in this work. In expression (1) b is the oscillator length$=1.006$ $A^{1/6}$ fm, σ is the Pauli spin matrix, and u_0 and u_1 are strength parameters (in MeV) which can be estimated from Refs. [38,39].

The core is described in the TQRM as an axially symmetrical or triaxial system, restricted to only one rigid shape, thus not allowing for softness or shape-coexistence. The static deformed harmonic oscillator (Nilsson) model with standard parameters [40] is used to generate single-particle states for the subsequent calculations. Pairing is treated in the usual BCS formalism (see, e.g., Ref. [41]). No neutron-proton pairing is included in the model at present, although this would be desirable for calculations involving $N=Z$ nuclei. The pairing strength parameters are taken as $G_{n0}=20.9$ MeV/nucleon and $G_{n1}=7.6$ MeV/nucleon for both the proton and neutron systems. This choice is suitable in the $A=70$ region as it gives pairing gaps (e.g., $\Delta_p=1.2$ MeV and $\Delta_n=1.19$ MeV) of about 90% of the odd-even mass differences expected in this mass region. The core moment of inertia is calculated to give a fixed value of the 2_1^+ state of the core. Two independent shapes for the core were employed. In particle-core coupling in the fp shell $E_{2_1^+}$ was taken to be 0.85 MeV. This value is reasonably close to the experimental energy of 2_1^+ states in ^{68}Se (0.854 MeV) and ^{72}Kr (0.710 MeV). The $g_{9/2}$ proton and neutron were coupled to a much more deformed core $E_{2_1^+}=0.23$ MeV which may be possibly associated with a coexisting deformed shape in either ^{68}Se or ^{72}Kr [42].

The TQRM model has been applied rather successfully before in the $A=80$ region for $N=Z+4$ (^{82}Y and ^{78}Rb [43]), for $N=Z+2$ (^{80}Y and ^{76}Rb) [44] and $N=Z$ (^{78}Y and ^{74}Rb) nuclei [17]. It was found that $N=Z+4$ nuclei were well described in the TQRM without use of any residual proton-neutron (p-n) interaction, while the CPL [37] p-n interaction had to be employed to explain the energy separation between the 1^- and 2^+ excited states and the 4^- ground state in ^{80}Y. No conclusive evidence for the role of the p-n interaction in the $N=Z$ ^{78}Y and ^{74}Rb nuclei could be drawn from the TQRM due to the complexity of the structure of their excited states. It is of interest to follow the question of the residual p-n interaction further to other nuclei in this region to obtain a clearer overall picture.

In order to explain the composite level scheme of ^{70}Br

TABLE II. Calculated structure of the ground state of ^{70}Br. Both odd proton and odd neutron occupy the same Nilsson state.

ϵ_2	State	Contribution
−0.18	3/2[312]	0.16
	5/2[303]	0.18
	1/2[312]	0.27
	1/2[310]	0.17
	3/2[301]	0.13
	1/2[301]	0.09
0.18	1/2[321]	0.08
	1/2[310]	0.13
	3/2[312]	0.12
	3/2[301]	0.24
	5/2[303]	0.23
	1/2[301]	0.20

(Fig. 3) two possible scenarios have to be considered. First, the 35th odd proton and neutron can occupy states in the fp shell at lower deformations or, second, they may occupy states in the $g_{9/2}$ shell at larger deformations. The observation of the 9^+ isomer at 2293 keV and the associated band indicates the presence of a $g_{9/2}$-based deformed structure. In contrast, the low-spin-excited states associated with the 0^+ ground state do not show evidence of a sizable deformation. Further, a developing collective structure is seen to be based on the $J^\pi=8^+$ state at 3028 keV. It is therefore likely that coexisting shapes will contribute to the composite spectrum of excited states of ^{70}Br, although their mixing is beyond the scope of the present model.

Starting with the low-spin region, both even-spin (up to 6^+) and odd-spin (up to 7^+) levels are calculated assuming the odd proton and odd neutron occupy states in the fp shell (see Table II). The lack of excited states observed below 934 keV can be explained as the effect of an attractive residual p-n interaction [Eq. (1)], with $u_0=-8.5$ MeV and $u_1=0$. The small influence of the spin-spin term in this case is a consequence of the spin saturation in the fp shell. Results of this calculation are presented in Fig. 11. The energy levels,

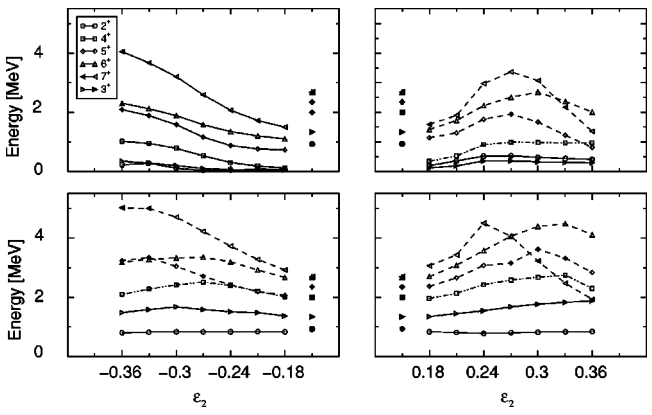

FIG. 11. Calculated energy levels of the ground-state structure as a function of deformation without (top panels) and with (bottom panels) the p-n interaction.

TABLE III. Ground-state quadrupole deformation β_2 of ^{68}Se, ^{72}Kr, and ^{70}Br as predicted in different nuclear models.

^{68}Se	^{72}Kr	^{70}Br	Ref.
0.287	−0.342	−0.340	FRDM [45]
−0.259	0.000		RMF [46]
−0.25	−0.29	−0.28	HFMF [47]
+0.40	+0.44		SMO2[a] [42]
−0.20	−0.25		

[a]Two coexisting minima are given.

shown as a function of deformation without the p-n interaction (top panels), are clearly at variance with experimental data. The bottom panels for which the pn interaction is included show the best agreement between experimental and calculated energies for $\epsilon_2=\pm 0.18$.

The TQRM does not give an unambiguous answer as to whether the core shape of the ^{70}Br ground state is oblate or prolate. The calculated level sequence is almost the same for both. For the prolate shape, the experimental energy of the 5_2^+ state at 2352 keV is fitted better, but the 7_1^+ state, measured at 2684 keV, is predicted too high. Transition probabilities, which are due to the very complex structure of the states involved (see Table II), also exhibit a weak dependence on the nuclear shape. Obtaining experimental transition probabilities from a later experiment to measure the lifetimes of excited states in ^{70}Br, while informative, would not, therefore, help to determine questions of nuclear shape in this case. However, the small moment of inertia needed to model the low-lying states in ^{70}Br would suggest in common with its even-even neighbors ^{68,70}Se and ^{72}Kr (see model predictions for the shapes of Se and Kr cores in Table III) that ^{70}Br also has an oblate ground state. While these systematic arguments provide a strong preference for an oblate shape, we note that a prolate solution cannot be rigorously excluded.

Calculation of the band associated with the isomeric 9^+ state at 2293 keV has been performed as a function of deformation. The best fit to experimental data was achieved for $\epsilon_2=-0.28$. In this case the prolate solution can be eliminated, as it predicts states with $J^\pi=7^+$ and 8^+ below the $J^\pi=9^+$ state. Extensive attempts to interpret the low-spin states in ^{70}Br as arising from structure built on the unfavored coupling $\Omega_p-\Omega_n$ of the $g_{9/2}$ proton and neutron as the 0^+ ground state did not yield agreement with experiment.

The calculation of the $9/2[404]_p\otimes 9/2[404]_n$ band itself is not sensitive to the residual p-n interaction. However, assuming that the two $J^\pi=8^+$ states at 3028 and, tentatively, at 3682 keV belong to the $g_{9/2}$ structure (which seems likely as the lowest $J^\pi=8^+$ states are predicted at ~ 5 MeV by the fp shell calculation) and that they correspond to the same core shape as the isomer, their relative position with respect to the isomer can be nicely reproduced using a repulsive p-n interaction with $u_0=5.60$ MeV and $u_1=0.63$ MeV. Here the spin-spin part of the interaction has to be taken into account as the $g_{7/2}$ orbital is not occupied.

As mentioned above, the TQRM cannot be used for a calculation of the absolute energy difference between struc-

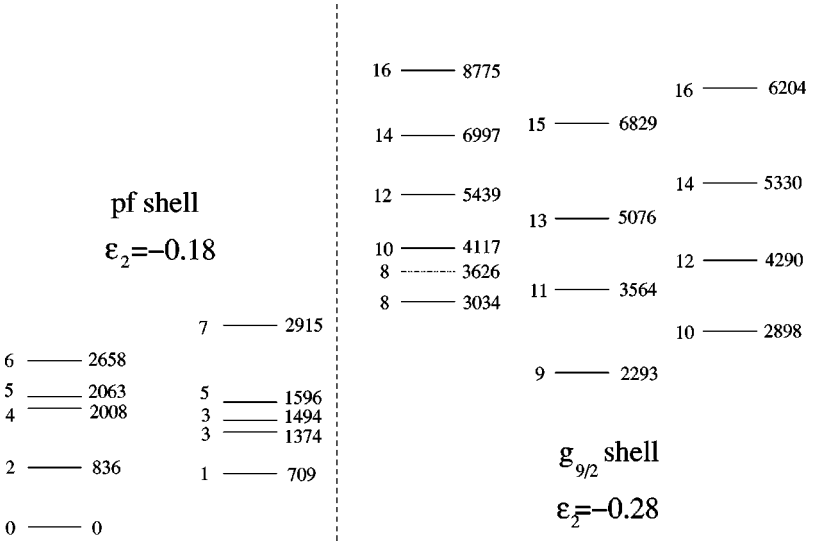

FIG. 12. Energy levels of ^{70}Br calculated within the TQRM formalism. The pf-ground-state-based and the $g_{9/2}$-isomeric-state-based structures are normalized, setting the energy of the calculated 9_1^+ state to the experimental value of 2293 keV. The levels marked with a dotted line have different structure from the others in the same column (see the text).

tures with different deformations. It follows that the position of the 9^+ isomer with respect to the ground state with a different single-particle makeup and different deformation cannot be calculated directly. However, it is instructive to normalize the energy spectrum of the $g_{9/2}$ system by fixing the energy of the 9^+ isomer to the experimental value of 2293 keV. The resulting composite energy spectrum is shown in Fig. 12, and exhibits good agreement with experiment.

As the structure of states of the $g_{9/2}$ system is much less complex than that of the pf system, it is interesting to investigate some states in more detail. First, the low-energy odd- and even-spin members of the band built on the isomer have a rather pure $9/2[404]_p \otimes 9/2[404]_n$ structure in the TQRM. The model also predicts that $\Delta I=2$ transitions should be more intense than $\Delta I=1$ transitions, in agreement with experiment where most of the latter were not observed (see Table IV). Clearly, the TQRM is not fully adequate to reproduce details of the band and its development to higher spins. The structure of the very high-spin states built on the isomer will be discussed in terms of the cranked Nilsson Strutinsky formalism in a later section.

Second, as illustrated in Table V, the 8_1^+ state at 3028 keV can be identified as a noncollective $9/2[404]_p \otimes 7/2[413]_n + 7/2[413]_p \otimes 9/2[404]_n$ band head. The calculated 8_2^+ state has a large component of the unfavored $\Omega_p - \Omega_n$ partner of the 9^+ isomer. This makes it less likely to be associated with the state observed at 3682 keV, despite the closeness in energy, because its decay mode is different from that expected for the unfavored band member. It would be very useful for model calculations if the unfavored band, or at least its 0^+ band head, were found experimentally.

In summary, the low-lying spectrum of excited states in ^{70}Br can be understood as consisting of two coexisting structures; the pf ground-state system at a rather low deformation with an axial symmetry, and an isomeric structure based on a coupling of the odd proton and odd neutron occupying the g_{92} orbital to a more deformed oblate core. Although not discussed above in detail, a departure from axial symmetry to triaxial core shapes did not improve the agreement with experiment in either the case of the ground state or the isomeric structures. The residual p-n interaction proved to be essential in reproducing correctly the low-lying energy spectrum of ^{70}Br in the TQRM.

TABLE IV. Calculated transition rates in the isomer band.

I_i	I_f	E^{γ}_{calc} (keV)	E^{γ}_{expt} (keV)	$T(E2)$ ps^{-1}	$T(M1)$ ps^{-1}
10	9	605	806	0.081	0.0061
11	9	1270	1255	0.182	0
12	11	726	984	0.305	0.0028
12	10	1391	1433	1.3	0
13	12	786	354	0.45	0.0046
13	11	1511	1338	3.1	0

C. Isospin invariant interacting boson model (IBM-4)

The IBM-4 [48] is the most elaborate version of the interacting boson model (IBM) of Arima and Iachello [49]. The bosons of IBM-4 are assigned an orbital angular momentum l which can be either $l=0$ or 2. In addition, they are labeled by an intrinsic spin s and an isospin t, for which the combinations $(s,t)=(0,1)$ and $(1,0)$ are retained. The bosons represent correlated fermion pairs and the choice of bosons is dictated by the requirement that they should describe nuclear excitations at low energy [48].

TABLE V. Structure of the 8_1^+ and 8_2^+ states at $\epsilon_2=-0.28$. Only components corresponding to different couplings of $\Omega_{p,n}$ higher than 5% are given.

State	Proton	Neutron	$\Omega_p+\Omega_n$	Ω_p-Ω_n
8_1^+	9/2[404]	7/2[413]	0.0	0.34
	7/2[413]	9/2[404]	0.0	0.57
8_2^+	9/2[404]	9/2[404]	0.0	0.60
	9/2[404]	7/2[413]	0.15	0.0
	7/2[413]	9/2[404]	0.17	0.0

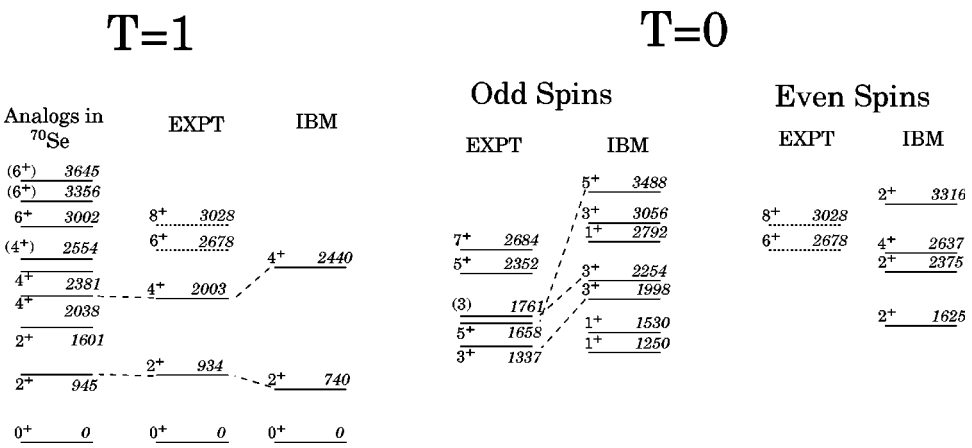

FIG. 13. Comparison of experimentally observed levels with the predictions of the IBM-4. The comparison is divided into $T=1$ states, including analogue states in ^{70}Se (left), $T=0$ states of odd spin (center), and $T=0$ states of even spin (right). Experimental states and their likely theoretical counterparts are joined by dashed lines as a guide to the eye. The experimental 6^+ and 8^+ states are shown in both the $T=1$ and 0 comparisons, since their isospin is not clearly established.

A recent application of the IBM-4 to nuclei in the first half of the 28–50 shell was presented in Ref. [50] in a fully microscopic approach. The boson energies and the boson–boson interactions are determined from a given shell-model Hamiltonian; this mapping is carried out for the two-particle and four-particle nuclei (here $A=58$ and 60 nuclei). Once the Hamiltonian is fixed in this way, predictions can be made for nuclei with more valence nucleons without introducing further parameters. This gives excellent results for ^{62}Ga [50], where a comparison with shell-model calculations can still be carried out.

The experimental levels in ^{70}Br as well as the $T=1$ analog levels taken from ^{70}Se are compared in Fig. 13 with the predictions of the IBM-4. While the theoretical counterparts for low-lying $T=0$ states in ^{70}Br are predicted by the model, they occur at much higher energy and this deviation grows as the spin increases. This is understandable as high-spin bosons are absent from this version of the IBM-4. Nevertheless, given that the model is microscopic and includes no free parameters, the agreement may be considered as encouraging. As regards the $T=1$ states, one notes the absence from the IBM-4 of a second 2^+ level seen in ^{70}Se at the experimental energy of $E_x=1601$ keV. This state can only be correctly reproduced after allowing a microscopically dictated boson-number dependence of the Hamiltonian. This deficiency of the current calculation for isovector states can thus presumably be traced back to the constancy of the boson Hamiltonian, and indicates the need to derive a boson-number dependence in the IBM-4. For a full comparison with the detailed spectroscopic information obtained in the present work, it will be necessary to also calculate transition rates and branching ratios in the framework of the IBM-4.

D. High-spin behavior of ^{70}Br: Cranked Nilsson-Strutinsky calculations

A topic of much recent interest has been the experimental observation of a delay in the location of the first back bending in the yrast line of the even-even $N=Z$ nuclei ^{72}Kr, ^{76}Sr, and ^{80}Zr relative to their $N=Z+2$ even-even neighbors [51–53]. While the experimental delay is now well established, the origins of this effect are presently unclear. Shape changes and enhanced pair fields have been suggested as possible causes of the delay. The pairing enhancements in $N=Z$ nuclei may arise from short-range np correlations either with $T=0$ or 1. However, the pairing fields are not very robust and the shell gaps that cause the shape polarizations can quench pairing, especially at high spin. In the odd-odd systems, the unpaired particles may further block pairing. Consequently, it is interesting to investigate ^{70}Br in a pairing-free calculation to act as a reference to locate where these correlations are no longer important.

In order to understand the structure of the asymptotic high-spin behavior of the bands in ^{70}Br found in the present work, calculations within the configuration-dependent cranked Nilsson-Strutinsky approach have been performed employing the formalism presented in Refs. [54,55]. The standard set of parameters [40] has been used for the Nilsson potential. Pairing correlations have been neglected in the present calculations—an assumption which may be considered realistic at high spin. The calculations indicate that the yrast line in the spin range $I\approx(15–25)\hbar$ is dominated by $(\pi=+,\alpha=1)$ odd-spin states. There are a number of competing $(\pi=+,\alpha=1)$ configurations shown in Fig. 14(a), which are yrast or close to yrast in the spin range of interest. The configurations are labeled by a shorthand notation $[p,n](\gamma_{av})$ where $p(n)$ is the number of $g_{9/2}$ protons (neutrons) and γ_{av} is the average γ deformation of the configuration. Since the potential energy surface is soft in the γ direction, we find configurations with the same occupation of high-j intruder orbitals in different local minima. To distinguish them, we employ an average gamma value, γ_{av}, as a shorthand label of the configurations.

The observed high-spin rotational sequence HB1 above $J=17$ appears to have regular spacing as expected for a collective band. It seems to be strongly populated. Collective bands are not predicted to be yrast in this calculation, as can be seen in Fig. 14—clearly a shortcoming. Possibly, the more irregular structures marked HB2 may be related to the non-collective states. Several non-yrast collective bands with two protons and two neutrons [2,2] and three protons and three neutrons [3,3] are predicted. Detailed comparison of experimental quantities such as $E-E_{RLD}$ [Fig. 14(b)], kinematic $J^{(1)}$ and dynamic $J^{(2)}$ moments of inertia [Fig. 15(a)] and alignments I [Fig. 15(b)] with theoretical predictions for these configurations strongly suggests the assignment of the $[3,3](\gamma\sim-20°)$ configuration for the $I=(15–25)\hbar$ states in

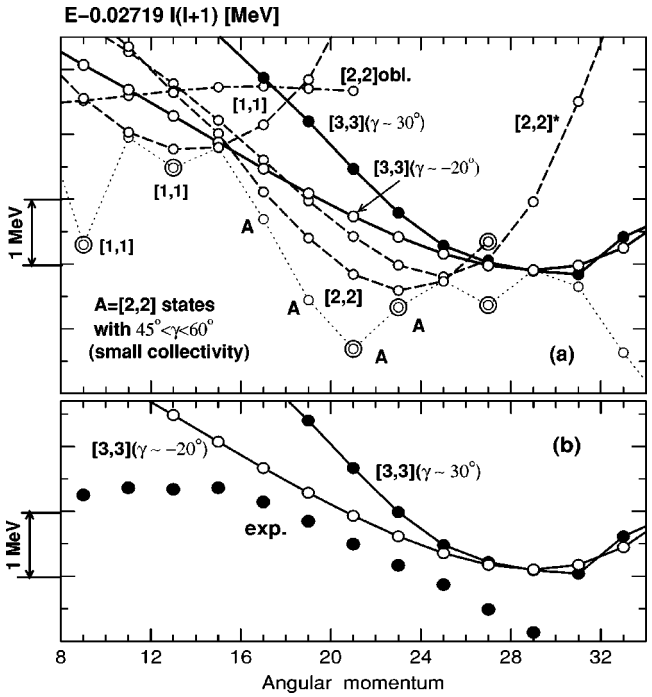

FIG. 14. (a) Excitation energies of the calculated ($\pi=+,\alpha=+1$) configurations as a function of angular momentum relative to a $I(I+1)$ rigid rotor reference. Calculated terminating states are circled. The yrast ($\pi=+,\alpha=+1$) line is indicated by the dotted line. (b) The same as in panel (a), but only for the experimental high-spin band, HB1, and the calculated [3,3]($\gamma\sim 30°$) and [3,3] $\times(\gamma\sim -20°)$ configurations.

band HB1. In the calculations, the [2,2] and [2,2]* configurations both lie below the [3,3]($\gamma\sim -20°$). We prefer to associate the latter configuration with the experimental band because of the better agreement of the $I(\omega)$ and (E-E_{RLD}) curves with the experiment [see Figs. 14(b) and 15(b)]. The [2,2] configurations have too small a dynamic moment of inertia, evident from the strong upbend around spin $24\hbar$ [see Fig. 14(a)] and the overly small slope for the angular momentum as a function of rotational frequency [see Fig. 15(b)]. Our interpretation raises the question of why [3,3] and not [2,2] configurations are observed. First we studied the sensitivity of the calculations to the input parameters. The relative position of the [3,3] and [2,2] configurations depends on the location of the $g_{9/2}$ orbitals relative to the negative parity orbitals which is, in turn, dependent on the parametrization of the Nilsson potential. In order to investigate this effect, we have also carried out calculations using the Nilsson parameter set from Ref. [56]. We find that, although the relative positions of the configurations are somewhat changed, the general structure remains the same.

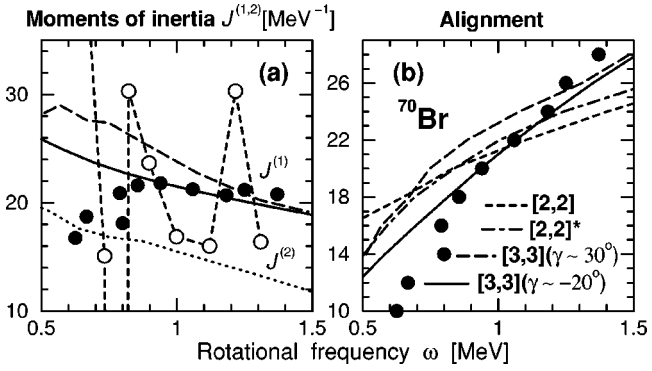

FIG. 15. Experimental and calculated kinematic and dynamic moments of inertia [panel (a)] and alignments [panel (b)]. The experimental alignment and kinematic moments of inertia are shown with filled circles, the dynamic moment of inertia with unfilled circles. The results of the calculations for different configurations [see panel (b) for the notation] are shown. The dotted line in panel (a) shows the calculated dynamic moment of inertia for the [3,3]($\gamma\sim -20°$) configuration.

The upbend seen around spin $J=15\hbar$ in HB1 can then be interpreted as a simultaneous alignment of two quasiprotons and two quasineutrons. Not surprisingly, these changes have a strong blocking effect and the pairing-free calculations begin to closely resemble the data. An upbend clearly seen in the dynamic moment of inertia at the highest observed rotational frequency [see Fig. 15(a)] may be interpreted as the crossing of the [3,3]($\gamma\sim -20°$) and [3,3]($\gamma\sim +30°$) configurations. Due to the similar structure of these two configurations and the rather small potential energy barrier between them, it is expected that there will be large matrix elements connecting the states in these two configurations.

An alternative scenario is that the [2,2] and [3,3] configurations are more strongly mixed than our calculations suggest, meaning that they interchange character very gradually forming the observed smooth rotational band. Such a mixing of the [2,2] and [3,3] configurations would represent the scattering of a proton and neutron on identical negative parity orbitals into identical $g_{9/2}$ orbitals, and vice versa. Such a pair has an isospin $T=0$, since the proton and neutron are in the same space-spin state. The observation of one smooth rotational band at high spin instead of the calculated distinct crossing between the [2,2] and [3,3] configurations may point to a strong scattering of $T=0$ pairs (i.e., $T=0$ pairing correlations) which are not taken into account in the calculations.

Clearly, more detailed data are needed to corroborate or refute these speculations. In particular, the observation of further high-spin bands and a determination of Q_t for the experimental band via lifetime measurements could clarify the situation, especially since the calculated Q_t is twice as large for the [3,3]($\gamma=-20°$) configuration as for the [2,2] configuration.

VII. CONCLUSIONS

We have begun to explore the rich structure of $T=0$ and $T=1$ states in ^{70}Br through two studies employing different reactions and channel selection techniques. As well as excited configurations based on the $J^{\pi}=0^{+}$ ground state, states above a previously known $J^{\pi}=9^{+}$ isomer have been observed and the excitation energy of the isomer has been fixed at 2293 keV. In all, 37 transitions have been located and placed in a decay scheme.

The aim of the present study was ''complete'' spectroscopy, i.e., finding all of the low-lying states. It is always

difficult to rigorously establish how successful such a search has been. Nevertheless, we have identified only one state in the first MeV of excitation. This does not seem to arise from an experimental lack of sensitivity, as we specifically designed an experiment which was unusually sensitive to the low-energy γ rays which are characteristic of the decay of bandheads in this region. None were found. This low level density can only be reproduced in particle rotor calculations for a modest deformation, which is most probably associated with an oblate shape and with an attractive long-range np interaction. The failure to observe any evidence of a doublet of states with $J=0$, $T=1$ and $J=1$, $T=0$ at low excitation appears to indicate that the $T=0$ n-p pairing strength is weak in comparison to the $T=1$ pairing strength.

The $J=9$ isomer has been located at 2293 keV. Particle rotor calculations clearly indicate the isomer must be oblate and associated with a sizeable deformation. For prolate solutions $J=7$ and 8 states are predicted to lie lower in energy than the $J=9$ state, thus removing the isomerism. The β decay of this isomer may provide a useful tool in locating oblate states in the daughter nucleus ^{70}Se.

The structure at very high spin has been interpreted in terms of a $[3,3](\gamma\sim-20°)$ configuration in an unpaired cranked Nilsson-Strutinsky formalism. The calculation reproduces the data very well in the regime above where both neutron and proton alignments have occurred and the effects of pairing may be neglected.

We find no evidence of $T=1$ states in the ground state band above $J=4$ and hence, question the recently claimed Coulomb energy shifts derived for ^{70}Br [24]. Moreover, we find no evidence of an isomer with $E_x=1214$ keV, as suggested by de Angelis *et al.* [24].

Clearly, a start has been made on investigating odd-odd nuclei in the $A=60$–90 region. The case of ^{70}Br, studied here, has turned out to be rather complicated for investigating np pairing as the issues of shape coexistence and shape mixing make the low-spin-level scheme very difficult to interpret. More data would help this disentanglement, especially lifetime data. However, it may well be the case that the main focus of this project; investigation of np correlations, can be better pursued in the heavier odd-odd isotopes ^{74}Rb and ^{78}Y for which prolate deformation is more firmly established

ACKNOWLEDGMENTS

R.W. and N.S.K. acknowledge support from EPSRC. R.W., N.S.K., R.M.C., and C.E.S. acknowledge receipt of a NATO grant. One of us (J.R.S.) wishes to acknowledge fruitful discussions and assistance of P. B. Semmes and financial support through U.S. Department of Energy Grant No. DE-FG02-94ER40834. This work was supported by U.S. Department of Energy Grant Nos. W-31-109-ENG38 and DE-FG02-95ER40934 and by National Science Foundation Grant No. PHY95-14157.

[1] P. von Brentano, A. F. Lisetskiy, A. Dewald, C. Friessner, A. Schmidt, I. Schneider, and N. Pietralla, Nucl. Phys. **A682**, 48c (2001).
[2] C. D. O'Leary *et al.*, Phys. Lett. B **459**, 73 (1999).
[3] A. Schmidt *et al.*, Phys. Rev. C **62**, 044319 (2000).
[4] A. F. Lisetskiy, R. V. Jolos, N. Pietralla, and P. von Brentano, Phys. Rev. C **60**, 064310 (1999).
[5] G. Morpurgo, Phys. Rev. **110**, 721 (1958).
[6] S. M. Vincent *et al.*, Phys. Lett. B **437**, 264 (1998).
[7] D. J. Dean, S. E. Koonin, K. Langanke, and P. B. Rudha, Phys. Lett. B **399**, 1 (1997).
[8] M. Honma, T. Mizusaki, and T. Otsuka, Phys. Rev. Lett. **77**, 3315 (1996).
[9] A. Stolz *et al.*, in *Selected Topics on N=Z Nuclei—Pingst 2000*, Lund, Sweden, 2001, edited by D. Rudolph and M. Hellstrom (University of Lund, Sweden, 2000), p. 113.
[10] J. Garces Narro, Phys. Rev. C **63**, 044307 (2001).
[11] M. Oinonen *et al.*, Phys. Lett. B **511**, 145 (2001).
[12] G. C. Ball *et al.*, Phys. Rev. Lett. **86**, 1454 (2001).
[13] D. Rudolph *et al.*, Nucl. Phys. **A694**, 132 (2001).
[14] R. Grzywacz *et al.*, Phys. Lett. B **429**, 247 (1998).
[15] R. Grzywacz *et al.*, Nucl. Phys. **A682**, 41c (2001).
[16] D. Rudolph *et al.*, Phys. Rev. Lett. **76**, 376 (1996).
[17] J. Uusitalo *et al.*, Phys. Rev. C **57**, 2259 (1998).
[18] R. H. Burch, C. A. Gagliardi, and R. E. Tribble, Phys. Rev. C **38**, 1365 (1988).
[19] B. Vosicki, T. Björnstad, L.C. Carraz, J. Heinemeier, and H.L. Ravn, Nucl. Instrum. Methods Phys. Res. **186**, 307 (1981).
[20] J. Döring *et al.*, *Selected Topics on N=Z Nuclei—Pingst 2000*, in Ref. [9], p. 131.
[21] A. Piechaczek *et al.*, Phys. Rev. C **62**, 054317 (2000).
[22] C. Borcan *et al.*, Eur. Phys. J. A **5**, 243 (1999).
[23] C. Borcan *et al.*, Eur. Phys. J. A **6**, 481 (1999).
[24] G. de Angelis *et al.*, Eur. Phys. J. A **12**, 51 (2001).
[25] D. G. Sarantites, Nucl. Instrum. Methods Phys. Res. A **381**, 418 (1996).
[26] D. G. Jenkins *et al.*, Phys. Rev. C **64**, 064311 (2001).
[27] D. Sohler *et al.*, Nucl. Phys. **A644**, 141 (1998).
[28] C. E. Svensson *et al.*, Nucl. Instrum. Methods Phys. Res. A **396**, 228 (1997).
[29] A. F. Lisetskiy *et al.*, Phys. Lett. B **512**, 290 (2001).
[30] J. Heese, K. P. Lieb, L. Lühmann, B. Wörmann, D. Alber, H. Grawe, J. Eberth, and T. Mylaeus, Z. Phys. A **325**, 45 (1986).
[31] S. M. Lenzi, Phys. Rev. C **60**, 021303(R) (1999).
[32] R.R. Chasman, Phys. Lett. B **524**, 81 (2002).
[33] S. M. Fischer, D. P. Balamuth, P. A. Hausladen, C. J. Lister, M. P. Carpenter, D. Seweryniak, and J. Schwartz, Phys. Rev. Lett. **84**, 4064 (2000).
[34] T. Mylaeus *et al.*, J. Phys. G **15**, L135 (1989).
[35] I. Ragnarsson and P. Semmes, Hyperfine Interact. **43**, 425 (1988).
[36] P. Semmes (private communication).
[37] J. P. Boisson, R. Piepenbring, and W. Ogle, Phys. Rep. **26**, 99 (1976).

[38] W. W. Daehnick, Phys. Rep. **96**, 6 (1983).
[39] R. Gross and A. Frenkel, Nucl. Phys. **A267**, 85 (1976).
[40] T. Bengtsson and I. Ragnarsson, Nucl. Phys. **A436**, 14 (1985).
[41] P. Moller and J.R. Nix, Nucl. Phys. **A536**, 20 (1992).
[42] J. Rikovska Stone, P. D. Stevenson, and M. R. Strayer (unpublished).
[43] P. C. Womble *et al.*, Phys. Rev. C **47**, 2546 (1993).
[44] J. Doring *et al.*, Phys. Rev. C **57**, 1159 (1998).
[45] P. Moller, J. R. Nix, W. D. Meyers, and W. J. Swiatecki, At. Data Nucl. Data Tables **59**, 185 (1995).
[46] G. A. Lalazissis, S. Raman, and P. Ring, At. Data Nucl. Data Tables **71**, 1 (1999).
[47] S. Goriely, F. Tondeur, and J. M. Pearson, At. Data Nucl. Data Tables **77**, 311 (2001).
[48] J. P. Elliott and J. A. Evans, Phys. Lett. **101B**, 216 (1981).
[49] F. Iachello and A. Arima, *The Interacting Boson Model* (Cambridge University, Cambridge, 1987).
[50] O. Juillet, P. Van Isacker, and D. D. Warner, Phys. Rev. C **63**, 054312 (2001).
[51] S. M. Fischer *et al.*, Nucl. Phys. **A682**, 35c (2001).
[52] S. M. Fischer *et al.*, Phys. Rev. Lett. **87**, 132501 (2001).
[53] N. S. Kelsall *et al.*, Phys. Rev. C **64**, 024309 (2001).
[54] A. V. Afanasjev and I. Ragnarsson, Nucl. Phys. **A591**, 387 (1995).
[55] A. V. Afanasjev, D. B. Fossan, G. J. Lane, and I. Ragnarsson, Phys. Rep. **322**, 1 (1999).
[56] D. Galeriu, D. Bucurescu, and M. Ivescu, J. Phys. G **12**, 329 (1986).